ResearchGate

See discussions, stats, and author profiles for this publication at: https://www.researchgate.net/publication/259808075

Indole-7-carbaldehyde thiosemicarbazone as a flexidentate ligand toward ZnII, CdII, PdII and PtII ions: Cytotoxic and apoptosis-inducing properties of the PtII complex

Article *in* Dalton Transactions · January 2014

DOI: 10.1039/c3dt53032a · Source: PubMed

CITATIONS
22

READS
149

5 authors, including:

Abeer A Ibrahim
Suliemani Polytechnic university
14 PUBLICATIONS **44** CITATIONS
SEE PROFILE

Pouya Hassandarvish
University of Malaya
78 PUBLICATIONS **2,455** CITATIONS
SEE PROFILE

Hamed Karimian
Taylor's University
51 PUBLICATIONS **1,225** CITATIONS
SEE PROFILE

Some of the authors of this publication are also working on these related projects:

Antibiotic Resistance of Pseudomonas aeruginosa Isolates from Patients in King Abdullah University Hospital in Jordan View project

Gastroprotective Activity of a synthetic compound View project

All content following this page was uploaded by Pouya Hassandarvish on 05 May 2014.

The user has requested enhancement of the downloaded file.

View Article Online
View Journal

Dalton Transactions

Accepted Manuscript

This article can be cited before page numbers have been issued, to do this please use: A. A. Ibrahim, H. Khaledi, P. Hassandarvish, H. Mohd Ali and H. Karimian, *Dalton Trans.*, 2013, DOI: 10.1039/C3DT53032A.

This is an *Accepted Manuscript*, which has been through the RSC Publishing peer review process and has been accepted for publication.

Accepted Manuscripts are published online shortly after acceptance, which is prior to technical editing, formatting and proof reading. This free service from RSC Publishing allows authors to make their results available to the community, in citable form, before publication of the edited article. This *Accepted Manuscript* will be replaced by the edited and formatted *Advance Article* as soon as this is available.

To cite this manuscript please use its permanent Digital Object Identifier (DOI®), which is identical for all formats of publication.

More information about *Accepted Manuscripts* can be found in the **Information for Authors**.

Please note that technical editing may introduce minor changes to the text and/or graphics contained in the manuscript submitted by the author(s) which may alter content, and that the standard **Terms & Conditions** and the **ethical guidelines** that apply to the journal are still applicable. In no event shall the RSC be held responsible for any errors or omissions in these *Accepted Manuscript* manuscripts or any consequences arising from the use of any information contained in them.

View Article Online
DOI: 10.1039/C3DT53032A

Indole-7-carbaldehyde thiosemicarbazone as a flexidentate ligand toward Zn^{II}, Cd^{II}, Pd^{II} and Pt^{II} ions: cytotoxic and apoptosis-inducing properties of the Pt^{II} complex.

Abeer A. Ibrahim,[a] Hamid Khaledi,*[a] Pouya Hassandarvish,[b] Hapipah Mohd Ali[a] and Hamed Karimian[b]

[a]*Department of Chemistry, University of Malaya, 50603 Kuala Lumpur, Malaysia*
[b]*Department of Molecular Medicine, University of Malaya, 50603 Kuala Lumpur, Malaysia*

Published on 26 November 2013. Downloaded by University of Malaya on 08/01/2014 07:12:34.

Dalton Transactions Accepted Manuscript

Summary

A new thiosemicarbazone (LH_2) derived from indole-7-carbaldehyde was synthesized and reacted with Zn^{II}, Cd^{II}, Pd^{II} and Pt^{II} salts.. The reactions with zinc and cadmium salts in 2:1 (ligand/metal) molar ratio afforded complexes of the type $MX_2(LH_2)_2$, (X = Cl, Br or OAc), in which the thiosemicabazone acts as a neutral *S*-monodentate ligand. In the presence of potassium hydroxide, the reaction of LH_2 with $ZnBr_2$ resulted in deprotonation of the thiosemicarbazone at the hydrazine and indole nitrogens to form $Zn(L)(CH_3OH)$. The reaction of LH_2 with K_2PdCl_4 in the presence of triethylamine, afforded $Pd(L)(LH_2)$ which contains two thiosemicabazone ligands: one being dianionic *N,N,S*-tridentate while the other one is neutral *S*-monodentate. When $PdCl_2(PPh_3)_2$ was used as the Pd^{II} ion source, $Pd(L)(PPh_3)$ was obtained. In a similar manner, the analogous platinum complex, $Pt(L)(PPh_3)$, was synthesized. The thiosemicarbazone in the latter two complexes behaves in a dianionic *N,N,S*-tridentate fashion. The platinum complex was found to have significant cytotoxicity toward four cancer cells lines, namely MDA-MB-231, MCF-7, HT-29, and HCT-116 but not toward the normal liver WRL-68 cell line. The

View Article Online
DOI: 10.1039/C3DT53032A

Published on 26 November 2013. Downloaded by University of Malaya on 08/01/2014 07:12:34.

apoptosis-inducing properties of the Pt complex was explored through fluorescence microscopy visualization, DNA fragmentation analysis and propidium iodide flow cytometry.

Introduction

Thiosemicarbazones constitute a class of ligands that have attracted a great deal of attention owing to their versatile coordination behavior toward metal ions.[1] Figure 1 presents a variety of coordination modes observed in thiosemicarbazone metal complexes. The coordination usually occurs through the sulfur atom and either the azomethine N atom to create a five-membered chelate ring (**1**),[2] or the hydrazine N atom to make a more strained four membered ring (**2**).[3,4] If the ligand contains a third donor site (D) appropriately located for coordination (*e.g.* salicylaldehyde thiosemicarbazone), a *D,N,S*-tricoordination normally takes place (**3**);[5-9] however examples are found in literature where the potential O donor atom from a salicylaldehyde thiosemicarbazone does not bind to the metal and the ligand shows an *N,S*-bidentate mode (**4** and **5**).[9-11] In addition, the *S*-donor atoms of thiosemicarbazones can bridge metal ions to form dinuclear,[12,13] or multinuclear metal complexes (**6**).[14-16] Other coordination modes observed in thiosemicabazones metal complexes include *S*-monodentate (**7**),[17-19] and *N*(thioamide),*S*-bidentate (**8**).[20] The applications of these metal complexes range from biological to material sciences fields. Examples are cytotoxic, antibacterial and antimalarial activities of thiosemicarbazone Pd^{II} and Pt^{II} complexes,[5-8,21] and non-linear optical properties associated with thiosemicarbazone Zn^{II} and Cd^{II} complexes.[17-19]

The present paper introduces a new thiosemicarbazone ligand (LH_2, Fig. 1) derived from indole-7-carbaldehyde. The structure of the molecule mimics that of salicylaldehyde thiosemicarbazone: both thiosemicarbazones have the third potential donor atom (D) linked to the carbonylic carbon *via* two intervening atoms; however, the third donor in LH_2 is the softer N atom vs. the harder O

Dalton Transactions Accepted Manuscript

View Article Online
DOI: 10.1039/C3DT53032A

atom in the salicylaldehyde derivative (**4** and **5**). The complexation behavior of LH_2 toward Zn^{II}, Cd^{II}, Pd^{II} and Pt^{II} is studied. Furthermore, the synthesized Pt^{II} complex was evaluated for its cytotoxicity and apoptosis-inducing properties.

Published on 26 November 2013. Downloaded by University of Malaya on 08/01/2014 07:12:34.

Results and discussion

The condensation reaction of indole-7-carboxaldehyde with thiosemicarbazide resulted in the formation of the corresponding thiosemicarbazone, LH_2. Similar to most thiosemicarbazones, the predominant form of LH_2 in both the solid state and solution is the thione tautomer (rather than the thiol tautomer). It is indicated by the absence of S-H band in the IR spectrum (at *ca.* 2700 cm^{-1}) and any signal attributable to the thiol proton in the ^1H NMR spectrum. The NN*H* signal of the thione is observed at $\delta = 11.25$ ppm.

The synthesized thiosemicarbazone, LH_2, was reacted with Zn, Cd, Pd and Pt salts under various conditions to afford the corresponding metal complexes in moderate to high yield (Scheme 1). Upon reaction of LH_2 with MX_2 (M = Zn or Cd; X = Cl, Br or OAc) in a ligand/metal ratio of 2:1, metal complexes with the formula of $MX_2(LH_2)_2$ were obtained. As revealed by X-ray crystallographic analysis, in the solid state structures of these complexes, LH_2 acts as a neutral *S*-monodentate ligand; however, the solution ^1H and ^{13}C NMR signals of the compounds do not show any shift from those of the free ligand suggesting that decomposition into the free ligand and metal salts in DMSO-d_6 solution occurs. In contrast, the reaction of LH_2 with $ZnBr_2$ in a 1:1 ratio and in the presence of KOH afforded a complex with the formula of $Zn(L)(CH_3OH)$. The ^1H NMR spectrum of this complex confirms the deprotonation of the indole N*H* and thioamide NN*H* of the ligand while its ^{13}C NMR spectrum shows an upfield shift of the *C*S signal (~ 4 ppm) and a downfield shift of the azomethine *C*HN signal (~ 4 ppm) from those in the spectrum

Dalton Transactions Accepted Manuscript

View Article Online
DOI: 10.1039/C3DT53032A

Published on 26 November 2013. Downloaded by University of Malaya on 08/01/2014 07:12:34.

of LH_2. Attempts to grow an X-ray quality crystal from this compound failed; however, based on elemental analysis and NMR spectroscopy the ligand in this compound is believed to act as a dianionic tridentate chelate, coordinating the metal atom through its sulfur, azomethine N and indole N atoms.

The reaction of LH_2 with K_2PdCl_4 in a 2:1 (ligand/metal) ratio and in the presence of triethylamine, led to the formation of $Pd(L)(H_2L)$. In agreement with the X-ray crystal structure, the solution ^1H and ^{13}C NMR spectra of this complex clearly show the existence of two types of the thiosemicarbazone ligand in the structure, one being doubly deprotonated while the other one is neutral. The upfield shift (5-6 ppm) of the two *C*S signals in the ^{13}C NMR spectrum of the complex compared to that of the free LH_2 suggests that the S atoms of both ligands remains coordinated to the Pd^{II} center in the DMSO-d_6 solution.

The reaction of LH_2 with $PdCl_2(PPh_3)_2$ in a 1:1 ratio and in the presence of triethylamine, yielded $Pd(L)(PPh_3)$. The platinum analog, $Pt(L)(PPh_3)$, was similarly obtained. The IR spectra of the two complexes closely resemble each other and agree with reported peaks for coordinated PPh_3 (e.g., 745, 691 and 537 for the Pd complex.[6] The solution ^1H and ^{13}C NMR spectra of the Pd complex do not show any characterizable species, suggesting the instability of the compound in DMSO solution. In contrast, the 1D- and 2D-NMR spectra of the Pt complex in DMSO-d_6 is in accordance with the solid state structure. In the ^1H NMR spectrum of the platinum complex the azomethine C*H*N signal (δ = 8.80 ppm) appears as a doublet due to the coupling with the phosphorus atom.[5,10] The phosphorus atom is also coupled with some of the carbon atoms so that their signals appear as doublets in the ^{13}C NMR spectrum. It is worth mentioning that the NMR solution of the Pt complex, kept at room temperature for a month, gave the same spectra as before, indicating the stability of the complex in DMSO solution.

Dalton Transactions Accepted Manuscript

View Article Online
DOI: 10.1039/C3DT53032A

Published on 26 November 2013. Downloaded by University of Malaya on 08/01/2014 07:12:34.

Crystal structure of $ZnBr_2(LH_2)_2$•2MeOH. The molecular structure of $ZnBr_2(LH_2)_2$ is shown in Fig. 2 and the selected bond lengths and angles are listed in Table S1†. Two thiosemicarbazone molecules, acting as neutral monodentate ligands, coordinate the metal center through their sulfur atoms. The two ligands are almost planar with r.m.s. deviation from the planes of S1 and S2 containing ligands being 0.0503 and 0.0284 Å respectively; the dihedral angle between the planes is 60.92(7)°. Two Br atoms complete the distorted tetrahedral geometry around the Zn atom with coordination angles in the range of 100.26(3)-113.80(2)°. The Zn-S bond lengths are comparable to those observed in similar structures,[17,19,22] and so are the Zn-Br distances.[19] There is intramolecular hydrogen bonding between hydrogens bonded to N3 and N7 and the Br ligands (Table S3†). Moreover, intermolecular N-H…Br interactions occur in the crystal to connect the adjacent molecules into chains along the *a* axis. The crystal structure contains methanol solvent molecules which are H-bonded to these chains.

Crystal structure of $CdCl_2(LH_2)_2$•MeOH. The molecular structure is depicted in Fig. 3 and Table S1† lists the selected bond lengths and angles. The structure is similar to that of the Zn complex. The thiosemicarbazone molecules are nearly planar (r.m.s. deviation = 0.0236 and 0.0715 Å for S1 and S2 containing ligands, respectively) and make a dihedral angle of 80.97(6)°. The Cd-S distances are compatible with those in similar structures.[18,23] Unlike the zinc complex structure, the intramolecular H-bonding occurs between the thioamide hydrogens, N4 and N8, and the halide ligands (Table S3†). The crystal packing shows interdigitating layers in the *bc* plane formed by intermolecular N-H…Cl interactions. Disordered solvent methanol molecules are N-H…O bonded to these layers.

Dalton Transactions Accepted Manuscript

View Article Online
DOI: 10.1039/C3DT53032A

Published on 26 November 2013. Downloaded by University of Malaya on 08/01/2014 07:12:34.

Crystal structure of $Cd(OAc)_2(LH_2)_2$. 2MeOH. The asymmetric unit of the crystal structure consists of two crystallographically independent Cd complexes and four methanol molecules. The two complexes have only slightly different geometrical parameters; the weighted r.m.s. fit for the superposition of the non-H atoms in both molecules is 0.103 Å. The structure of one of the complex molecules is depicted in Fig. 4 and selected bond lengths and angles are listed in Table S1†. The Cd^{II} atom is coordinated by two thiosemicarbazone molecules which behave as neutral S-donor monodentate ligands. One monodentate and one bidentate acetate groups complete a five-coordinate metal complex. The coordination geometry can be determined using the index $\tau = (\beta-\alpha)/60$ where β is the largest angle and α is the second one around the metal center.[24] For an ideal square pyramidal geometry $\tau = 0$, while it is 1 for a perfect trigonal bipyramidal geometry. In the present structure τ computes to 0.23 which indicates a distorted square-pyramidal geometry. The r.m.s deviation from planarity for the S1 and S2 containing ligands are 0.068 and 0.095 Å, respectively, and the two planes make a dihedral angle of 4.96(12)°. There is intramolecular hydrogen bonding between thioamide nitrogens N4 and N8 and the monodentate acetate ligand (Table S3†). In the crystal, the complexes are connected through intermolecular N-H…O and N-H…N interactions to form infinite chains along the crystallographic *a* direction. The methanol solvate molecules are H-bonded to the formed chains.

Crystal structure of $Pd(L)(HL_2)$. The crystal structure of $Pd(L)(HL_2)$ is depicted in Fig. 5. The Pd center is coordinated by two different thiosemicarbazone ligands, one of them being dianionic *N,N',S*-tridentate, while the other one acts as a neutral *S*-monodenate ligand. The two ligands are almost planar with r.m.s. deviation from planarity for their non-H atoms of 0.087 and 0.034 Å for the tridentate and monodentate ligands respectively. The two planes make a dihedral

Dalton Transactions Accepted Manuscript

View Article Online
DOI: 10.1039/C3DT53032A

Published on 26 November 2013. Downloaded by University of Malaya on 08/01/2014 07:12:34.

angle of 77.67(3)°. The selected bond lengths and angles for the structure are gathered in Table S2†. The longer S1-C10 bond length than S2-C20 distance points out the higher thiolic character of the tridentate ligand compared to the monodentate ligand. The two ligands differ also in their configuration about N3-C10 (*Z*) and N8-C20 (*E*) bonds, in keeping with what was observed in the structures of similar Pd complexes.[25,26] The metal atom is in a distorted square-planar geometry and is displaced by 0.0575 (6) Å out of the coordination plane (N1/N2/S1/S2). In the crystal, pairs of the metal complex molecules are doubly connected through N8-H8A…N3 hydrogen bonding into centro-symmetric dimers (Table S3†). The resulting dimers are connected to each other *via* C-H…π and N-H…π interactions to form a three-dimensional network with voids of the size of 331 $Å^3$ wherein disorder solvent molecules reside.

Crystal structure of Pd(L)(PPh_3)•DMF. The molecular structure of Pd(L)(PPh_3) and the labeling scheme is depicted in Fig. 6. The doubly deprotonated thiosemicarbazone ligand coordinates the Pd atom in an *N,N',S*-tridentate manner to create five- and six-memebred chelate rings. A triphenylphosphine group occupies the fourth coordination site, making a square-planar palladium complex with the metal atom being 0.0236 Å out of the coordination plane, N1/N2/S1/P1. The ligand is almost planar with an r.m.s. deviation of 0.0536 Å. Table S2† lists the selected bond lengths and angles for the structure. While the Pd-N1 and Pd-S distances are comparable to those in Pd(L)(LH_2), the Pd-N2 distance in the present structure is 0.0431 Å longer than that in the former structure. This can be attributed to the *trans*-influence of the PPh_3 ligand as was observed in similar palladium complex structures.[7,8] In the crystal, pairs of the metal complex molecule are connected into centro-symmetric dimers through N4-H4B…N3 hydrogen bonds and these are linked *via* C-H…π interactions to form a three-dimensional

Dalton Transactions Accepted Manuscript

View Article Online
DOI: 10.1039/C3DT53032A

Published on 26 November 2013. Downloaded by University of Malaya on 08/01/2014 07:12:34.

polymeric structure (Table S3†). In the crystal, disordered DMF solvate molecules exist as hydrogen bond acceptors in N4-H4A…O interactions.

Crystal structure of Pt(L)(PPh_3)•0.75MeOH. The molecular structure of the platinum(II) complex (Fig. 7) resembles that of Pd(L)(PPh3). The planar thiosemicarbazone (r.m.s deviation = 0.0812 Å) is doubly deprotonated and coordinated to the platinum atom through its indolic N, azomethine N and thioamide S atoms to form a five- and a six-membered chelate ring. A triphenylphosphine ligand at the fourth coordination site completes a distorted square-planar Pt^{II} complex; the metal center is displaced from the coordination plane, N1/N2/S1/P1, by 0.0578 Å. Table S2† compiles the selected bond lengths and angles for the structure. The Pt-P is slightly shorter and Pt-N2 slightly longer than corresponding bond lengths in similar structures.[27,28] In the crystal, the molecules are connected through C-H…π interactions to form hexagonal channels along the *c*-axis (void size = 264 $Å^3$) within which there is no evidence for included solvent (Fig. 8). The outer-shell of the channel is solvated by the partially occupying methanol molecules (Table S3†).

Cytotoxicity assay

Preliminary cytotoxicity screening for LH_2 and its Pd and Pt complexes against four cancer cell lines, revealed significant activity for Pt(L)PPh_3. Table 1 lists the IC_{50} values of the platinum complex after treating the cell lines for 24, 48 and 72 h. As shown by the results, for 24 h treatments the IC_{50} values lie between 2.08-22.97 μM. These values dropped when the treatments were prolonged, thus the IC_{50} values for 48 h treatments range from 1.49 to 3.34 μM

Dalton Transactions Accepted Manuscript

View Article Online
DOI: 10.1039/C3DT53032A

Published on 26 November 2013. Downloaded by University of Malaya on 08/01/2014 07:12:34.

and for 72 h treatments are between 0.77-2.77 μM. The effect of the platinum complex on normal liver cell lines (WRL-68) was also examined. As shown in Fig. 9, minimal toxicity was observed at the concentrations below 40 μM, attesting to cancer-selective cytotoxicity of $Pt(L)(PPh_3)$ at low doses. For the sake of comparison, cells were also treated with cisplatin, a clinical anticancer drug. As presented in Table 1, compared to cisplatin, $Pt(L)(PPh_3)$ exerted higher or comparable cytotoxicity against the cancer cell lines and higher selectivity for the cancer cells over normal cells.

Table 1 IC50 (μM) values ± SEM of Pt(L)(PPh3) and cisplatin on different cancer cell lines

		24 hours	48 hours	72 hours
MDA-MB-231	$Pt(L)(PPh_3)$	22.97 ± 4.13	3.34 ± 0.18	2.27 ± 0.28
	Cisplatin	18.09 ± 1.32	16.37 ± 0.65	15.64 ± 0.77
MCF-7	$Pt(L)(PPh_3)$	2.23 ± 0.13	1.49 ± 0.04	0.77 ± 0.045
	Cisplatin	14.76 ± 0.58	11.89 ± 0.71	9.13 ± 0.62
HT-29	$Pt(L)(PPh_3)$	2.08 ± 0.12	1.74 ± 0.29	0.94 ± 0.02
	Cisplatin	72.68±0.92	36.71 ± 3.48	5.76 ± 1.49
HCT-116	$Pt(L)(PPh_3)$	3.71 ± 0.10	2.41 ± 0.24	1.52 ± 0.04
	Cisplatin	38.73±8.23	23.95 ± 5.18	5.76 ± 1.49
WRL-68	$Pt(L)(PPh_3)$	52.58 ± 0.71	48.01 ± 0.49	48.53 ± 0.67
	Cisplatin	> 80	13.58 ± 2.34	10.32 ± 1.62

Dalton Transactions Accepted Manuscript

View Article Online
DOI: 10.1039/C3DT53032A

Published on 26 November 2013. Downloaded by University of Malaya on 08/01/2014 07:12:34.

Apoptosis assay

Apoptosis induction is an anti-proliferative mechanism by which the cancer cells undergo programmed death. Cells undergoing apoptosis are characterized by morphological and biochemical changes including cell shrinkage, chromatin condensation and DNA fragmentation. Based on the results of the *in vitro* cytotoxicity assay for $Pt(L)PPh_3$, it was considered worthwhile to explore the apoptotic properties of the compound. Apoptosis in the four cancer cell lines was examined through fluorescence microscopy visualization, DNA fragmentation analysis and propidium iodide flow cytometry.

Fluorescence microscopy visualization. Apoptotic cells exhibit increased plasma membrane permeability to certain fluorescent dyes. Acridine orange (AO)/propidium iodide (PI) is a fluorochrome mixture for nuclear staining which enables distinction between viable, apoptotic and necrotic cells. In this work, the four cancer cell lines were subjected to AO/PI staining after treatment with respective IC_{50} concentrations of $Pt(L)PPh_3$ for 48 h. Fluorescence microscopy reveals that in all the cancer lines the platinum complex induced cell death mainly *via* apoptosis (Fig. 10).

Fluorochrome-labelled Annexin V staining is another way for microscopic visualization of the apoptotic cells. Normal cells have the phospholipid phosphatidylserine (PS) on their inner-leaflet of the membranes, but upon undergoing apoptosis, PS becomes exposed on the external side of the cellular membrane. Annexin V binds to cell membranes containing exposed PS, thus labelled annexin V can be used to detect apoptotic cells at early stages. In this study FITC-annexin V was applied to target the apoptotic cells after treatment of the cancer cells with IC_{50} concentrations of $Pt(L)PPh_3$ for 48 h. The fluorescence microscopic examination of the treated

Dalton Transactions Accepted Manuscript

View Article Online
DOI: 10.1039/C3DT53032A

Published on 26 November 2013. Downloaded by University of Malaya on 08/01/2014 07:12:34.

cells when compared to those grown under the control conditions attest to the binding of FITC-annexin V to the externalized PS in the treated cells, thus induction of apoptosis by the platinum complex in the four cancer cell lines (Fig. 11).

DNA Fragmentation analysis. The degradation of nuclear DNA into nucleosomal units is a biochemical feature of apoptosis. To evaluate the apoptotic DNA fragmentation in the cancer cells, the four cell lines were incubated with the corresponding IC_{50} values of $Pt(L)PPh_3$ for 48 h. The cells were then lysed, the nuclear DNA was extracted, and subjected to gel electrophoresis. Inspection of the electrophoretic profiles revealed a ladder formation (fragments range from 400 to 1000 bp), attesting to the occurrence of apoptosis (Fig. 12).

Cell cycle analysis. The DNA content of cells duplicates during the S phase, therefore cells in the G_0 and G_1 phases (before the S phase) have unreplicated DNA, while those in the G_2 and M phases (after the S phase) have replicated DNA. Analysis of cell cycles by flow cytometry enables us to distinguish and quantify the cells in different phases of the cell cycle. On the flow cytometry DNA histograms cells with degraded and thus hypodiploid DNA are represented in so-called "sub-G_0/G_1" peaks therefore, sub-G_0/G_1 is a specific marker of cell death by apoptosis.[28] Flow cytometry analysis of the four cancer cell lines after treatments with respective IC_{50} concentrations of the $Pt(L)PPh_3$ for 24 and 48 h was carried out. The DNA histograms (Fig. 13) suggest that the HCT-116 and MDA-MB-231 cell cycles were arrested in the G_0/G_1 phase whereas the HT-29 and MCF-7 cell cycle arrests happened in the S phase. Moreover, the histogram shows gradual increases in the populations of sub-G_0/G_1cells during the incubation

Dalton Transactions Accepted Manuscript

View Article Online
DOI: 10.1039/C3DT53032A

periods. Overall flow cytometry suggests the induction of apoptosis by the platinum complex in the cancer cells through G_0/G_1 or S phase cell cycle arrest.

Conclusion

LH_2, a new thiosemicarbazone whose structure resembles that of salicylaldehyde thiosemicarbazone, is a polydentate ligand having flexidentate character toward metal ions. In the examples in this study it exhibits two coordination modes, *i.e. S*-monodentate (in its neutral form) and *N,N,S*-tridenate (in a dianionic form). The latter creates a five- and a six-membered chelate ring with the metal ion. It would appear that the coordination mode is ruled by the basicity of the reaction medium, ligand/metal ratio and the identity of the metal salt. The indole N atom is either deprotonated and coordinated to the metal center or is intramoleculary H-bonded to the azomethine N atom. In all the examples, regardless of the charge and denticity of the ligand and the coordination geometry of the complex, the thiosemicarbazone ligands keep their planarity.

The platinum complex introduced in this article has shown a remarkable and cancer-selective cytotoxicity against a variety of cell lines as inferred from the MTT-based IC_{50} values and different apoptotic assay methods thus, can be considered as a potential anticancer drug.

Experimental

Materials and Measurements

Indole-7-carbaldehyde was purchased from Sigma-Aldrich Company. Ethanol was distilled prior to use. The IR spectra were obtained using a Perkin–Elmer Spectrum 400 ATR-FTIR

Published on 26 November 2013. Downloaded by University of Malaya on 08/01/2014 07:12:34.
Dalton Transactions Accepted Manuscript

View Article Online
DOI: 10.1039/C3DT53032A

Published on 26 November 2013. Downloaded by University of Malaya on 08/01/2014 07:12:34.

spectrometer. The NMR spectra were recorded with a JEOL Lambda 400 MHz FT-NMR spectrometer.

Synthesis

LH_2. A mixture of indole-7-carbaldehyde (1.45 g, 10 mmol) and thiosemcarbazide (0.91 g, 10 mmol) in ethanol (25 mL) containing a few drops of acetic acid was refluxed for 3 h. The solution was then partially evaporated followed by addition of distilled water to precipitate the yellowish product. It was filtered, washed with 30% aqueous ethanol and dried over silica gel. Yield: 1.9 g, 87%. Anal. Calcd for $C_{10}H_{10}N_4S$: C, 55.02; H, 4.62; N, 25.67; S, 14.69. Found: C, 55.13; H, 4.45; N, 25.33%. IR (ATR): 3445, 3407, 3383, 3234, 3145, 1610, 1526, 1363, 1335, 1290, 944, 897, 825, 795, 728, 712 cm^{-1}. ^1H NMR (DMSO-d_6): δ 6.53 (dd, 1H, Ar-*H*); 7.06 (t, 1H, Ar-*H*); 7.17 (d, 1H, Ar-*H*); 7.37 (t, 1H, Ar-*H*); 7.65 (d, 1H, Ar-*H*); 8.25 (s, 1H, NH_2); 8.28 (s, 1H, NH_2); 8.33 (s, 1H, C*H*N); 10.98 (s, 1H, indole N*H*); 11.25 (s, 1H, NN*H*) ppm.^{13}C NMR (DMSO-d_6): δ 102.42, 117.59, 119.63, 123.60, 126.19, 127.03, 129.23, 131.17 (*Ar*); 146.47 (*C*HN); 177.64 (*C*S) ppm.

$ZnBr_2(LH_2)_2$. A solution of $ZnBr_2.2H_2O$ (0.13 g, 0.5 mmol) in methanol (5 mL) was added to a solution of LH_2 (0.218 g, 1 mmol) in the same solvent (10 mL). The mixture was refluxed for 4 h and then set aside at room temperature for 5 days whereupon crystals of $ZnBr_2(LH_2)_2.2MeOH$ were formed. After the structure determination by X-ray crystallography, the crystals were ground and dried at 50 °C for the other analysis purposes. Yield: 0.225 g, 68%. Anal. Calcd. For $C_{20}H_{20}Br_2N_8S_2Zn$: C, 36.30; H, 3.05; N, 16.93. Found: C, 36.69; H, 3.13; N, 16.77%. IR (ATR): 3441, 3329, 3227, 1603, 1546, 1375, 1337, 1284, 950, 814, 792, 725, 717 cm^{-1}.

Dalton Transactions Accepted Manuscript

View Article Online
DOI: 10.1039/C3DT53032A

Published on 26 November 2013. Downloaded by University of Malaya on 08/01/2014 07:12:34.

$CdCl_2(LH_2)_2$. A solution of $CdCl_2.2H_2O$ (0.11 g, 0.5 mmol) in methanol (5 mL) was added to a methanolic solution (10 mL) of LH_2 (0.218 g, 1 mmol). The mixture was refluxed for 4 h, then set aside at room temperature for one day whereupon X-ray quality crystals of $CdCl_2(LH_2)_2$. MeOH were formed. After the structure determination, the crystals were ground and dried at 50 °C. Yield: 0.216 g, 79%. Anal. Calcd. For $C_{20}H_{20}CdCl_2N_8S_2$: C, 38.75; H, 3.25; N, 18.08. Found: C, 38.57; H, 3.36; N, 17.98%. IR (ATR): 3399, 3285, 3187, 1605, 1549, 1371, 1337, 1287, 953, 893, 815, 797, 731, 715 cm^{-1}.

$Cd(OAc)_2(LH_2)_2$. A solution of $Cd(OAc)_2.2H_2O$ (0.133 g, 0.5 mmol) in methanol (10 mL) was added to a solution of H_2L (0.218 g, 1 mmol) in the same solvent (10 mL). The mixture was refluxed for 4 h and then set aside at room temperature overnight whereupon X-ray quality crystals of $Cd(LH_2)_2(OAc)_2$. 2MeOH were obtained. After the crystal structure determination, the crystals were ground and dried at 50 °C and used for further analysis. Yield: 0.169 g, 51%. Anal. Calcd. For $C_{24}H_{26}CdN_8O_4S_2$: C, 43.21; H, 3.93; N, 16.80. Found: C, 42.66; H, 4.66; N, 16.54%. IR (ATR): 3415, 3265, 3159, 1610, 1542, 1372, 1339, 1294, 829, 793, 730, 693 cm^{-1}.

Zn(L)(CH_3OH). To a solution of LH_2 (0.218 g, 1 mmol) and KOH (0.14 g, 2.5 mmol) in methanol (10 mL), a solution of $ZnBr_2.2H_2O$ (0.261 g, 1 mmol) in the same solvent (10 mL) was added and the mixture was stirred at room temperature for 24 h. The resulting precipitate was filtered, washed with 50% aqueous ethanol and dried over silica gel. Yield: 0.23 g, 74%. Anal. Calcd. For $C_{20}H_{20}Br_2N_8S_2Zn$: C, 42.12; H, 3.86; N, 17.86. Found: C, 42.13; H, 3.42; N, 18.05%. IR (ATR): 3424, 3252, 3142, 1604, 1538, 1372, 1330, 1280, 896, 824, 795, 734 cm^{-1}. ^1H NMR (DMSO-d_6): δ 3.13 (d, 3H, C*H*$_3$OH); 4.12 (q, 1H, CH$_3$O*H*); 6.29 (s, 2H, N*H*$_2$); 6.37 (d, 1H, Ar-*H*); 6.83 (t, 1H, Ar-*H*); 7.03 (d, 1H, Ar-*H*); 7.49 (d, 1H, Ar-*H*); 7.51 (d, 1H, Ar-*H*); 8.40 (s, 1H,

Dalton Transactions Accepted Manuscript

View Article Online
DOI: 10.1039/C3DT53032A

Published on 26 November 2013. Downloaded by University of Malaya on 08/01/2014 07:12:34.

C*H*N) ppm. ^{13}C NMR (DMSO-d_6): δ 49.13 (*C*H_3OH); 100.74, 116.52, 119.15, 122.16, 123.72, 131.53, 137.74, 140.61 (*Ar*); 150.22 (*C*HN); 173.23 (*C*S) ppm.

Pd(L)(H$_2$L). A solution of K_2PdCl_4 (0.163 g, 0.5 mmol) in methanol (5 mL) was added to a solution of LH_2 (0.218 g, 1 mmol) in the same solvent (10 mL) followed by addition of a few drops of triethylamine. The mixture was refluxed for 5 h, and then set aside at room temperature for one day whereupon brownish crystals of the product were formed. X-ray crystallographic analysis of the crystals showed inclusion of disordered solvent molecules in the crystal, therefore for the other analysis purposes the crystals were ground and dried at 50 °C. Yield: 0.194 g, 72%. Anal. Calcd. For $C_{20}H_{18}N_8PdS_2$: C, 44.41; H, 3.35; N, 20.71. Found: C, 44.41; H, 3.69; N, 20.32%. IR (ATR): 3420 (sh), 3309, 1600, 1550, 1506, 1304, 1231, 793, 732 cm^{-1}. ^{1}H NMR (DMSO-d_6): δ 6.48 (d, 1H, Ar-*H*); 6.57 (dd, 1H, Ar-*H*); 6.62 (br, 2H, NH_2); 6.95 (t, 1H, Ar-*H*); 7.10 (t, 1H, Ar-*H*); 7.30 (d, 1H, Ar-*H*); 7.38 (d, 1H, Ar-*H*); 7.43 (m, 1H, Ar-*H*); 7.73 (m, 3H, Ar-*H*); 8.38 (s, 1H, C*H*N); 8.53 (s, 1H, C*H*N); 9.04 (s, 1H, NH_2); 9.31 (s, 1H, NH_2); 11.14 (s, 1H, indole N*H*); 12.18 (s, 1H, NN*H*) ppm. ^{13}C NMR (DMSO-d_6): δ 101.69, 102.69, 116.59, 116.83, 117.59, 119.74, 124.82, 124.89, 125.89, 127.21, 127.40, 129.34, 129.93, 131.30, 133.45, 135.29 (*Ar*); 147.52, 151.63 (*C*HN); 171.68, 172.92 (*C*S) ppm.

Pd(L)(PPh$_3$). A solution of *trans*-$PdCl_2(PPh_3)_2$ (0.702 g, 1 mmol) in methanol (10 mL) was added to a solution of LH_2 (0.218 g, 1 mmol) in the same solvent (10 mL) followed by addition of a few drops of triethylamine. The mixture was refluxed for 5 h and then set aside at room temperature for a few days whereupon the orange crystals of the product appeared. The crystals were ground and dried at 50 °C. Yield: 0.480 g, 82%. Anal. Calcd. For $C_{28}H_{23}N_4PPdS$: C, 57.49; H, 3.96; N, 9.58. Found: C, 57.23; H, 4.04; N, 9.27. %. IR (ATR): 3442 (w), 3320 (w), 1603, 1556, 1517, 1435, 1306, 1233, 792, 745, 691, 537 cm^{-1}.

Dalton Transactions Accepted Manuscript

View Article Online
DOI: 10.1039/C3DT53032A

Published on 26 November 2013. Downloaded by University of Malaya on 08/01/2014 07:12:34.

X-ray quality crystals of Pd(L)(PPh_3).DMF were obtained from a DMF solution of the complex on standing for four days at room temperature.

Pt(L)(PPh_3). A solution of *cis*-$PtCl_2(PPh_3)_2$ (0.791 g, 1 mmol) in methanol (10 mL) was added to a solution of LH_2 (0.218 g, 1 mmol) in the same solvent (10 mL) followed by addition of a few drops of triethylamine. The mixture was refluxed for 6 h and then set aside at room temperature overnight whereupon X-ray quality crystals of the product were obtained. After the crystal structure determination, the crystals were washed with 50% aqueous ethanol, ground and dried at 50 °C. Yield: 0.512 g, 76%. Anal. Calcd. For $C_{28}H_{23}N_4PPtS$: C, 49.92; H, 3.44; N, 8.32. Found: C, 49.69; H, 3.04; N, 8.28%. IR (ATR): 3441(w), 3318 (w), 1603, 1556, 1520, 1434, 1304, 1233, 791, 743, 689, 538 cm^{-1}.^{1}H NMR (DMSO-d_6): δ 6.13 (d, 1H, Ar-*H*); 6.65 (br s, 2H, N*H*$_2$); 6.72 (d, 1H, Ar-*H*); 7.10 (t, 1H, Ar-*H*); 7.47-7.55 (m. 9H, Ar-*H*); 7.61 (d, 1H, Ar-*H*); 7.68-7.73 (dd, 6H, Ar-*H*); 7.75-7.77 (d, 1H, Ar-*H*); 8.80 (d, 1H, C*H*N) ppm. ^{13}C NMR (DMSO-d_6): δ 102.75, 117.21, 117.57, 125.86, 127.48, 128.72 (*Ar*); 129.13 (d, *J* [^{31}P-^{13}C] = 42.04 Hz, *Ar*); 130.14, 130.75 (*Ar*); 132.21 (d, *J* [^{31}P-^{13}C] = 23 Hz, *Ar*); 135.15 (d, *J* [^{31}P-^{13}C] = 45.96 Hz, *Ar*), 139.90 (d, *J* [^{31}P-^{13}C] = 26.84 Hz, *Ar*); 147.70 (*C*HN); 171.28 (d, *J* [^{31}P-^{13}C] = 45.96 Hz, *C*S) ppm.

X-ray Crystallography

Diffraction data were measured with a Bruker SMART Apex II CCD area-detector diffractometer (graphite-monochromated Mo-*K*α radiation, λ = 0.71073 Å). The orientation matrix, unit-cell refinement, and data reduction were all handled by the Apex2 software (SAINT integration, SADABS absorption correction).[30] The structures were solved using direct or Patterson methods in the program SHELXS-97 and were refined by the full matrix least-squares

Dalton Transactions Accepted Manuscript

View Article Online
DOI: 10.1039/C3DT53032A

Published on 26 November 2013. Downloaded by University of Malaya on 08/01/2014 07:12:34.

method on F^2 with SHELXL-97.[31] All the non-hydrogen atoms were refined anisotropically. The structure of Pd(L)(LH_2) contains disordered solvent molecules which could not be satisfactorily modeled. The data were therefore treated with the SQUEEZE routine of PLATON.[32] For Drawings of the molecules were produced with XSEED.[33] Crystal data and refinement details are summarized in Tables S4 and S5†.

Cytotoxicity assay

Cell culture. The cell lines were provided by Faculty of Medicine, University of Malaya. All the cells were cultured in either Dulbecco's modified Eagle's medium (DMEM) or RPMI 1640 supplemented with 10% fetal bovine serum (Sigma Aldrich) and L-glutamine at 37 °C in a 5% CO_2 humidified atmosphere.

MTT cytotoxixity test. MTT (3-(4,5-dimethylthiazol-2-yl)-2,5-diphenyltetrazolium bromide) assay was carried out as described by Mosmann,[34] with some modifications. The cells were seeded into 96-well plates (5000 cells/well) and allowed to adhere overnight. Pt(L)PPh_3 was pre-dissolved in dimethyl sulfoxide (DMSO) and diluted to the desired concentrations (eight concentrations, 0.39-50 µg/mL), such that the final concentrations of DMSO did not exceed 0.5%. Each cell line was treated with the test compound solutions (three wells on a plate for each concentration) for 24, 48 and 72 h. Treated and untreated cells were inspected qualitatively using an inverted light microscope (100 X). Then, 10 µl of MTT (5 mg/mL) was added to each well and the plates were incubated at 37 °C for 4 h. The media was then gently aspirated, and 100 µl DMSO was added to dissolve the formazan crystals. The amount of formazan product was measured spectrophotometrically at 570 nm using a microplate reader (Power Wave X 340). The concentration of the test compound required for 50% inhibition of cell growth (IC_{50}) was determined by interpolation of regression analysis.

Dalton Transactions Accepted Manuscript

View Article Online
DOI: 10.1039/C3DT53032A

Published on 26 November 2013. Downloaded by University of Malaya on 08/01/2014 07:12:34.

Apoptosis detection with fluorescence microscopy

AO/PI staining assay. The cancer cells were seeded in a 25 mL culture-flask (1×10^6 cells/mL) and treated with the Pt complex at the corresponding IC_{50} concentrations for 48 h (control cells were treated with 0.5% DMSO vehicle). The cells were then washed with phosphate buffered saline (PBS) and suspended in 500 μL of PBS followed by addition of a 1:1 mixture of AO (10 μg/ml) and PI (10 μg/ml). A drop of the suspension was placed on a glass slide and covered with a cover slip. Images of the cells were taken by a UV-fluorescence microscope within 30 min.

Annexin V staining. The cancer cells (1×10^6 cells) were seeded on a chamber slide and were treated with the respective IC_{50} concentrations of the Pt complex for 48 h (control cells were treated with 0.5% DMSO vehicle). The media was then removed and the slide was washed with PBS. Treated and control cells were exposed to FITC-annexin V for 15 min according to the manufacturer's protocol (BD Pharmingen, USA). After a 488 nm excitation, green fluorescence (emission at 515 nm) was visualized by an inverted fluorescence microscope.

DNA Fragmentation analysis

The cancer cells were seeded in a 25 mL culture-flask (1×10^6 cells/mL) and treated with the respective IC50 concentrations of the test compound for 48 h (control cells were treated with 0.5% DMSO vehicle). The cells were then washed with PBS. The treated and control cells were washed with PBS and harvested. Cellular DNA was extracted using a Genomic DNA purification kit (Promega, Madison, WI). The DNA fragments were then separated by a 1.5% agarose gel electrophoresis at 50 V for 1.5 h. The Gels were then stained with ethidium bromide and visualized on a UV-illuminator.

Dalton Transactions Accepted Manuscript

View Article Online
DOI: 10.1039/C3DT53032A

Published on 26 November 2013. Downloaded by University of Malaya on 08/01/2014 07:12:34.

Cell cycle analysis

Cell cycle analysis was carried out by propidium iodide flow cytometry as described elsewhere.[35] Briefly, the cancer cells (1×10^6) were seeded in three culture flaks and were treated with the respective IC_{50} concentrations of the Pt complex for 24 h and 48 h. The cells were then washed with PBS, suspended in 90% ethanol and kept overnight (4°C). The pellets were further washed with PBS and suspended in PBS at 37 °C. 25 µl of RNase A (10 µg/ml) and 50 µl of propidium iodide (10 µg/ml) were added to the mixture and the cells were incubated at 37°C for 30 min. The distribution of the cell cycle was measured by a FACsCANTO II flow cytometer, and the data were analyzed with Prism 5.

Electronic supplementary information (ESI):

CCDC reference numbers 939908-939913 for $ZnBr_2(LH_2)_2$.2MeOH, $CdCl_2(LH_2)_2$.MeOH, $Cd(OAc)_2(LH_2)_2$.2MeOH, Pd(L)(LH_2), Pd(L)(PPh_3).DMF and Pt(L)(PPh_3).0.75 MeOH, X-ray crystallographic files in CIF format, tables for the selected geometrical parameters for the crystal structures, tables for crystal data and refinement parameters, ^1H, ^{13}C NMR, HSQC and HMBC spectra of selected compounds.

Acknowledgments

We would like to thank Maysam Hafezparast Maradat, Shahram Golbabapour, Maryam Zahedi Fard and Javad Paydar from Faculty of Medicine, University of Malaya for their assistance with the biological data collection and analysis. Financial Support from the University of Malaya (HIR Grant Number UM.C/625/1/HIR/151, UMRG Grant Number RG066/12BIO and PPP

Dalton Transactions Accepted Manuscript

View Article Online
DOI: 10.1039/C3DT53032A

Grant Number PV048/2012A) and the Center for Natural Products and Drug Research, CENAR, (FL001-13BIO) is highly appreciated.

References

1 T. S. Lobana, R. Sharma, G. Bawa and S. Khanna, *Coord. Chem. Rev*., 2009, **253**, 977.

2 P. Paul, S. Datta, S. Halder, R. Acharyya, F. Basuli, R. J. Butcher, S. M. Peng, G. H. Lee, A. Castineiras, M. G. B. Drew and S. Bhattacharya, *J. Mol. Catal. A: Chem.,* 2011, **344**, 62.

3 F. Basuli, S. M. Peng and S. Bhattacharya, *Inorg. Chem*., 2000, **39**, 1120.

4 D. Mishra, S. Naskar, M. G. B. Drew and S. K. Chattopadhyay, *Inorg. Chim. Acta*, 2006 **359**, 585.

5 P. Kalaivani, R. Prabhakaran, F. Dallemer, P. Poornima, E. Vaishnavi, E. Ramachandran, V. V. Padma, R. Renganathan and K. Natarajan, *Metallomics*, 2012, **4**, 101.

6 S. Halder, S. M. Peng, G. H. Lee, T. Chatterjee, A. Mukherjee, S. Dutta, U. Sanyal and S. Bhattacharya, *New J. Chem*., 2008, **32**, 105.

7 P. Chellan, N. Shunmoogam-Gounden, D. T. Hendricks, J. Gut, P. J. Rosenthal, C. Lategan, P. J. Smith, K. Chibale and G. S. Smith, *Eur. J. Inorg. Chem.,* 2010, 3520.

8 R. Prabhakaran, S. V. Renukadevi, R. Karvembu, R. Huang, J. Mautz, G. Huttner, R. Subashkumar and K. Natarajan, *Eur. J. Med. Chem.*, 2008, **43**, 268.

9 R. Prabhakaran, K. Palaniappan, R. Huang, M. Sieger, W. Kaim, P. Viswanathamurthi, F. Dallemer and K. Natarajan, *Inorg. Chim. Acta*, 2011, **376**, 317.

Published on 26 November 2013. Downloaded by University of Malaya on 08/01/2014 07:12:34.

Dalton Transactions Accepted Manuscript

View Article Online
DOI: 10.1039/C3DT53032A

Published on 26 November 2013. Downloaded by University of Malaya on 08/01/2014 07:12:34.

10 P. Kalaivani, R. Prabhakaran, E. Ramachandran, F. Dallemer, G. Paramaguru, R. Renganathan, P. Poornima, V. V. Padma and K. Natarajan, *Dalton Trans.*, 2012, **41**, 2486.

11 L. Latheef, E. Manoj and M. R. P. Kurup, *Polyhedron,* 2007, **26**, 4107.

12 A. Nunez-Montenegro, R. Carballo and E. M. Vazquez-Lopez, *Polyhedron*, 2009, **28**, 3915.

13 M. D. Revenko, P. N. Bourosh, E. F. Stratulat, I. D. Corja, M. Gdaniec, Y. A. Simonov and F. Tuna, *Russ. J. Inorg. Chem*., 2009, **54**, 530.

14 D. Kovala-Demertzi, N. Kourkoumelis, M. A. Demertzis, J. R. Miller, C. S. Frampton, J. K. Swearingen and D. X. West, *Eur. J. Inorg. Chem*., 2000, 727.

15 P. N. Yadav, M. A. Demertzis, D. Kovala-Demertzi, A. Castineiras and D. X. West, *Inorg. Chim. Acta*, 2002, **332**, 204.

16 F. Hueso-Urena, N. A. Illan-Cabeza, M. N. Moreno-Carretero, A. L. Penas-Chamorro and R. Faure, *Inorg. Chem. Commun.,* 1999, **2**, 323.

17 Y. P. Tian, W. T. Yu, C. Y. Zhao, M. H. Jiang, Z. G. Cai and H. K. Fun, *Polyhedron,* 2002, **21**, 1217.

18 Y. P. Tian, C. Y. Duan, C. Y. Zhao, X. Z. You, T. C. W. Mak and Z. Y. Zhang, *Inorg. Chem.,* 1997, **36**, 1247.

19 C. Y. Duan, Z. H. Liu, Y. C. Shi and X. Z. You, *J. Coord. Chem.*, 1999, **47**, 433.

20 Y. Han, J. Zhang, F. Han, Z. Zhang, L. Weng and X. Zhou, *Organometallics*, 2009, **28**, 3916.

Dalton Transactions Accepted Manuscript

View Article Online
DOI: 10.1039/C3DT53032A

Published on 26 November 2013. Downloaded by University of Malaya on 08/01/2014 07:12:34.

21 K. O. S. Ferraz, G. M. M. Cardoso, C. M. Bertollo, E. M. Souza-Fagundes, N. Speziali, C. L. Zani, I. C. Mendes, M. A. Gomes and H. Beraldo, *Polyhedron*, 2011, **30**, 315.

22 P. Souza, L. Sanz, V. Fernandez, A. Arquero, E. Gutierrez and A. Monge, *Z. Naturforsch., B: Chem. Sci.*, 1991, **46**, 767.

23 C. Y. Duan, Y. P. Tian, C. Y. Zhao, X. Z. You and T. C. W. Mak, *Polyhedron*, 1997, **16**, 2857.

24 A. W. Addison, T. N. Rao, J. Reedijk, V. J. Rijn and G. C. Verschoor, *J. Chem. Soc., Dalton Trans.,* 1984, 1349.

25 L. Papathanasis, M. A. Demertzis, P. N. Yadav, D. Kovala-Demertzi, C. Prentjas, A. Castineiras, S. Skoulika and D. X. West, *Inorg. Chim. Acta,* 2004, **357**, 4113.

26 V. V. Bon, S. I. Orysyk, V. I. Pekhnyo and S. V. Volkov, *J. Mol. Struct*., 2010, **984**, 15.

27 S. Halder, R. J. Butcher and S. Bhattacharya, *Polyhedron*, 2007, **26**, 2741.

28 T. S. Lobana, G. Bawa, G. Hundal and M. Zellere, *Z. Anorg. Allg. Chem*., 2008, **634**, 931.

29 W. G. Telford, L. E. King and P. J. Fraker, *Cytometry*, 1992, **13**, 137.

30 Bruker APEX2 and SAINT, Bruker AXS Inc., Madison, Wisconsin, USA, 2007.

31 G. M. Sheldrick, *Acta Crystallogr., Sect. A,* 2008, **64**, 112.

32 A. L. Spek, *PLATON*, Utrecht University, Utrecht, The Netherlands, **2010**.

33 L. J. Barbour, *J. Supramol. Chem.,* 2001, **1**, 189.

34 T. Mosmann, *J. Immunol. Methods*, 1983, **65**, 55.

35 D. Jain, N. Patel, M. Shelton, A. Basu, R. Roque and W. Siede, Cancer Chemother. Pharmacol., 2010, **66**, 945.

Dalton Transactions Accepted Manuscript

View Article Online
DOI: 10.1039/C3DT53032A

Text for the table of contents entry

The Pt(II) complex of a new series of thiosemicarbazone complexes exhibits cancer-selective cytotoxicity

Published on 26 November 2013. Downloaded by University of Malaya on 08/01/2014 07:12:34.

Dalton Transactions Accepted Manuscript

View Article Online
DOI: 10.1039/C3DT53032A

Published on 26 November 2013. Downloaded by University of Malaya on 08/01/2014 07:12:34.

List of figure captions

Fig. 1 Various coordination modes observed in metal complexes of thiosemcarbazone ligands (**1-8**); the chemical diagram of LH_2

Scheme 1. Reactions of LH_2 with the selected metal salts

Fig. 2 The molecular structure of ZnBr2(LH2)2 with thermal ellipsoids drawn at the 30% probability level. Methanol solvate molecules are not shown.

Fig. 3 The molecular structure of $CdCl_2(LH_2)_2$ with thermal ellipsoids drawn at the 30% probability level. Methanol solvate molecules are not shown.

Fig. 4 The molecular structure and atom labeling scheme of $Cd(OAc)_2(LH_2)_2$ (25% probability ellipsoids). Methanol solvate molecules are not shown.

Fig. 5 The molecular structure of $Pd(L)(HL_2)$ with thermal ellipsoids drawn at 30% probability level.

Fig. 6 The molecular structure of $Pd(L)(PPh_3)$ with thermal ellipsoids drawn at 50% probability level. The DMF solvate molecules are not shown.

Dalton Transactions Accepted Manuscript

View Article Online
DOI: 10.1039/C3DT53032A

Fig. 7 The molecular structure and atom labeling scheme of $Pt(L)(PPh_3)$ (50% probability ellipsoids). Methanol solvate molecules are not shown.

Fig. 8 Crystal packing view of $Pt(L)(PPh_3).0.75MeOH$, showing channels along the *c*-axis. Hydrogen bonds are depicted as red dashed lines.

Fig. 9 Cytotoxicity effect of $Pt(L)(PPh_3)$ on normal liver WRL-68 cells

Fig. 10 Fluorescent microscopy of AO/PI stained cancer cells. The first row shows the cells without any treatment and the second row shows the cells after treatment with IC_{50} concentrations of $Pt(L)PPh_3$ for 48 h. Cells with intact membrane are stained green. Apoptotic cells appear in orange-yellow and the necrotic cells are stained red.

Fig. 11 Fluorescence microscopy of the cancer cells stained by FITC-annexin V. The first row shows the cells without any treatment and the second row shows the cells treated with $Pt(L)PPh_3$ at IC_{50} concentraions for 48 h. FITC-annexin V positive cells show bright green fluorescence.

Fig. 12 Gel electrophoresis of apoptotic DNA fragmentation. Lane A: 1000 bp molecular weight marker; lane B: untreated MDA-MB-231 cells; lane C: treated MDA-MB-231 cells; lane D: untreated MCF-7 cells; lane E: treated MCF-7 cells; lane F: untreated HT-29 cells; lane G: treated HT-29 cells; lane H: untreated HCT-116 cells; lane I: treated HCT-116 cells.

Published on 26 November 2013. Downloaded by University of Malaya on 08/01/2014 07:12:34.

Dalton Transactions Accepted Manuscript

View Article Online
DOI: 10.1039/C3DT53032A

Fig. 13 Flow cytometric analysis of cell cycle distribution in the four cancer cell lines treated with IC_{50} concentrations of $Pt(L)PPh_3$ for 24 and 48 h. Data were shown as Mean ± SEM. * $\rho <$ 0.05 *vs*. controls.

Published on 26 November 2013. Downloaded by University of Malaya on 08/01/2014 07:12:34.

Dalton Transactions Accepted Manuscript

View Article Online
DOI: 10.1039/C3DT53032A

Published on 26 November 2013. Downloaded by University of Malaya on 08/01/2014 07:12:34.

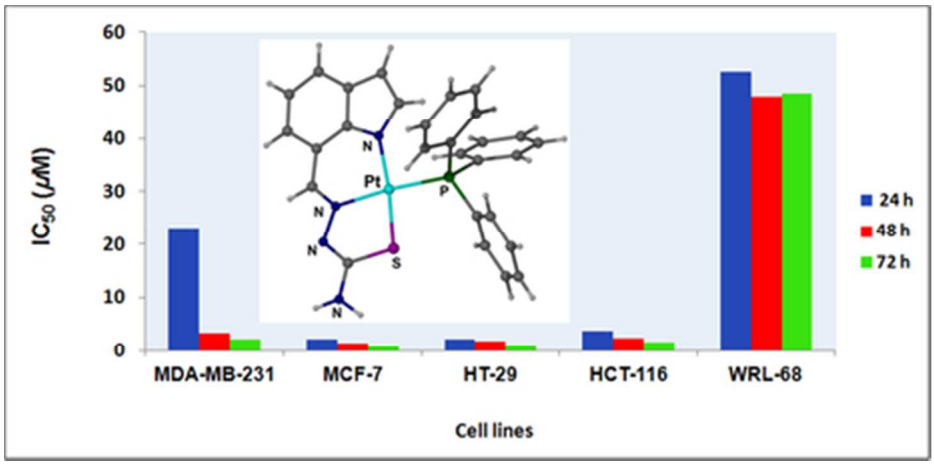

The Pt(II) complex of a new series of thiosemicarbazone complexes exhibits cancer-selective cytotoxicity
39x19mm (300 x 300 DPI)

Dalton Transactions Accepted Manuscript

View Article Online
DOI: 10.1039/C3DT53032A

Published on 26 November 2013. Downloaded by University of Malaya on 08/01/2014 07:12:34.

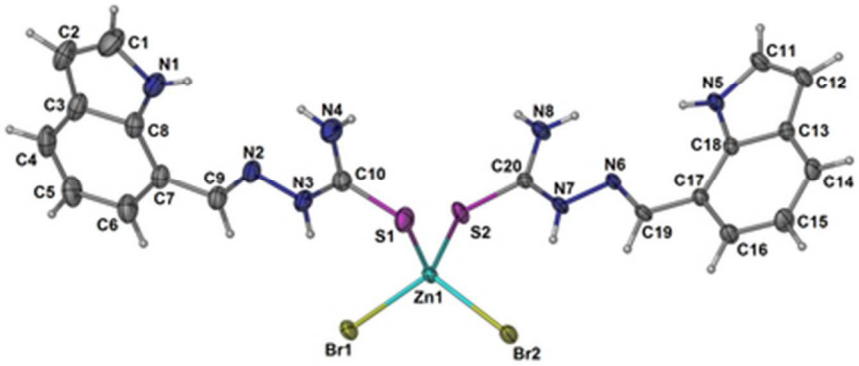

Fig. 2 The molecular structure of ZnBr2(LH2)2 with thermal ellipsoids drawn at the 30% probability level. Methanol solvate molecules are not shown.
36x16mm (300 x 300 DPI)

Dalton Transactions Accepted Manuscript

View Article Online
DOI: 10.1039/C3DT53032A

Published on 26 November 2013. Downloaded by University of Malaya on 08/01/2014 07:12:34.

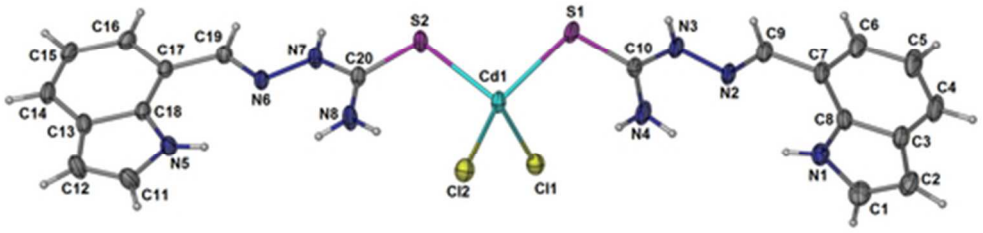

Fig. 3 The molecular structure of CdCl2(LH2)2 with thermal ellipsoids drawn at the 30% probability level. Methanol solvate molecules are not shown.
43x22mm (300 x 300 DPI)

Dalton Transactions Accepted Manuscript

View Article Online
DOI: 10.1039/C3DT53032A

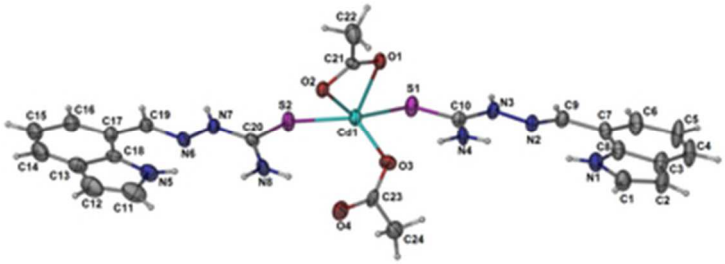

Fig. 4 The molecular structure and atom labeling scheme of Cd(OAc)2(LH2)2 (25% probability ellipsoids). Methanol solvate molecules are not shown.
30x11mm (300 x 300 DPI)

Published on 26 November 2013. Downloaded by University of Malaya on 08/01/2014 07:12:34.

Dalton Transactions Accepted Manuscript

View Article Online
DOI: 10.1039/C3DT53032A

Published on 26 November 2013. Downloaded by University of Malaya on 08/01/2014 07:12:34.

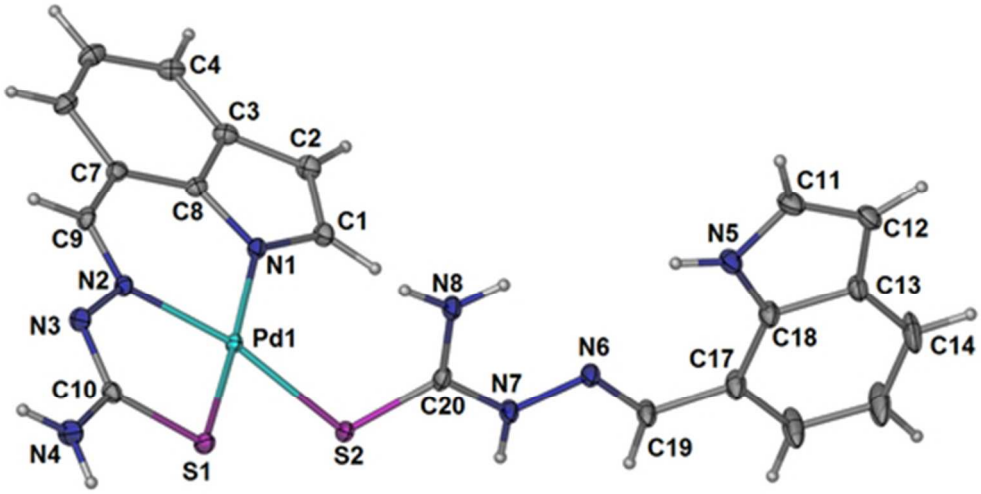

Fig. 5 The molecular structure of Pd(L)(HL2) with thermal ellipsoids drawn at 30% probability level.
42x21mm (300 x 300 DPI)

Dalton Transactions Accepted Manuscript

View Article Online
DOI: 10.1039/C3DT53032A

Published on 26 November 2013. Downloaded by University of Malaya on 08/01/2014 07:12:34.

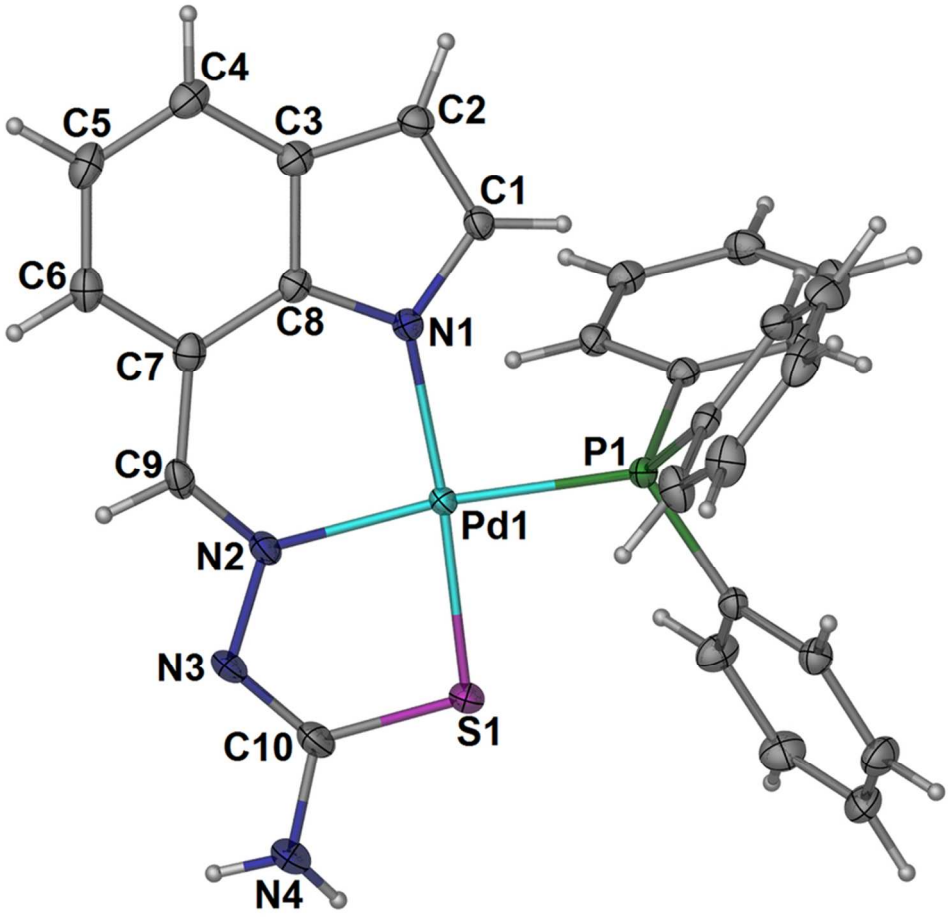

Fig. 6 The molecular structure of Pd(L)(PPh3) with thermal ellipsoids drawn at 50% probability level. The DMF solvate molecules are not shown.
81x79mm (300 x 300 DPI)

Dalton Transactions Accepted Manuscript

View Article Online
DOI: 10.1039/C3DT53032A

Published on 26 November 2013. Downloaded by University of Malaya on 08/01/2014 07:12:34.

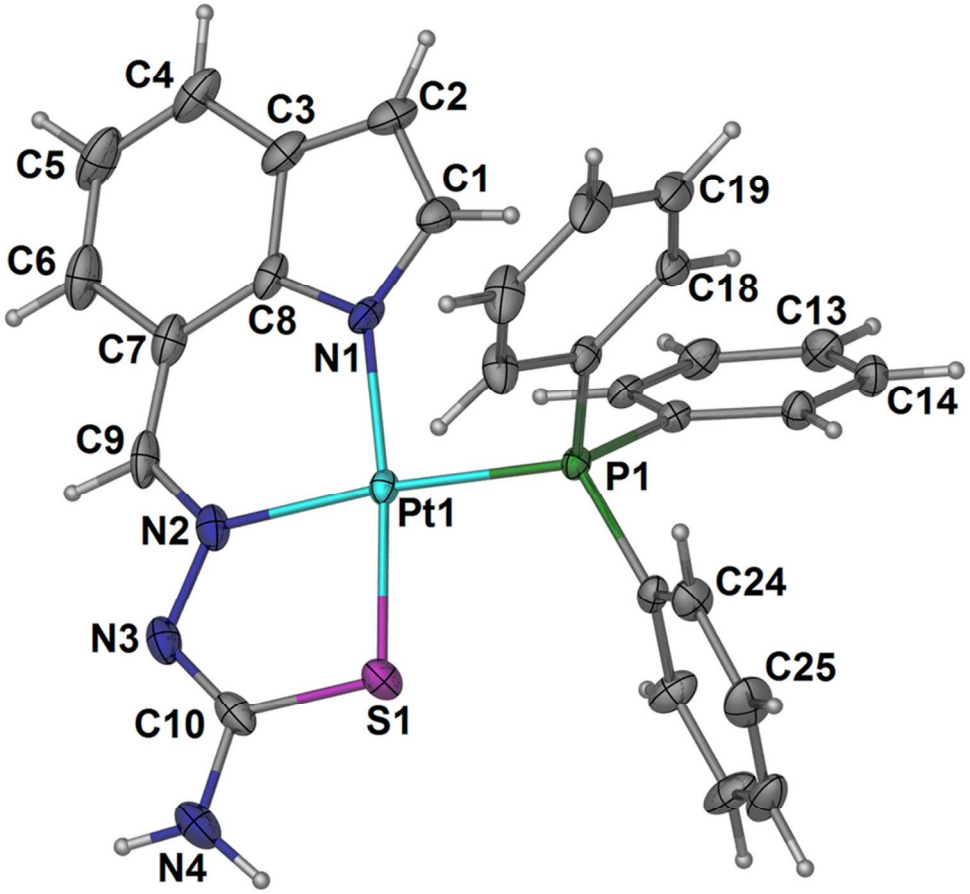

Fig. 7 The molecular structure and atom labeling scheme of Pt(L)(PPh3) (50% probability ellipsoids). Methanol solvate molecules are not shown.
78x73mm (300 x 300 DPI)

Dalton Transactions Accepted Manuscript

View Article Online
DOI: 10.1039/C3DT53032A

Published on 26 November 2013. Downloaded by University of Malaya on 08/01/2014 07:12:34.

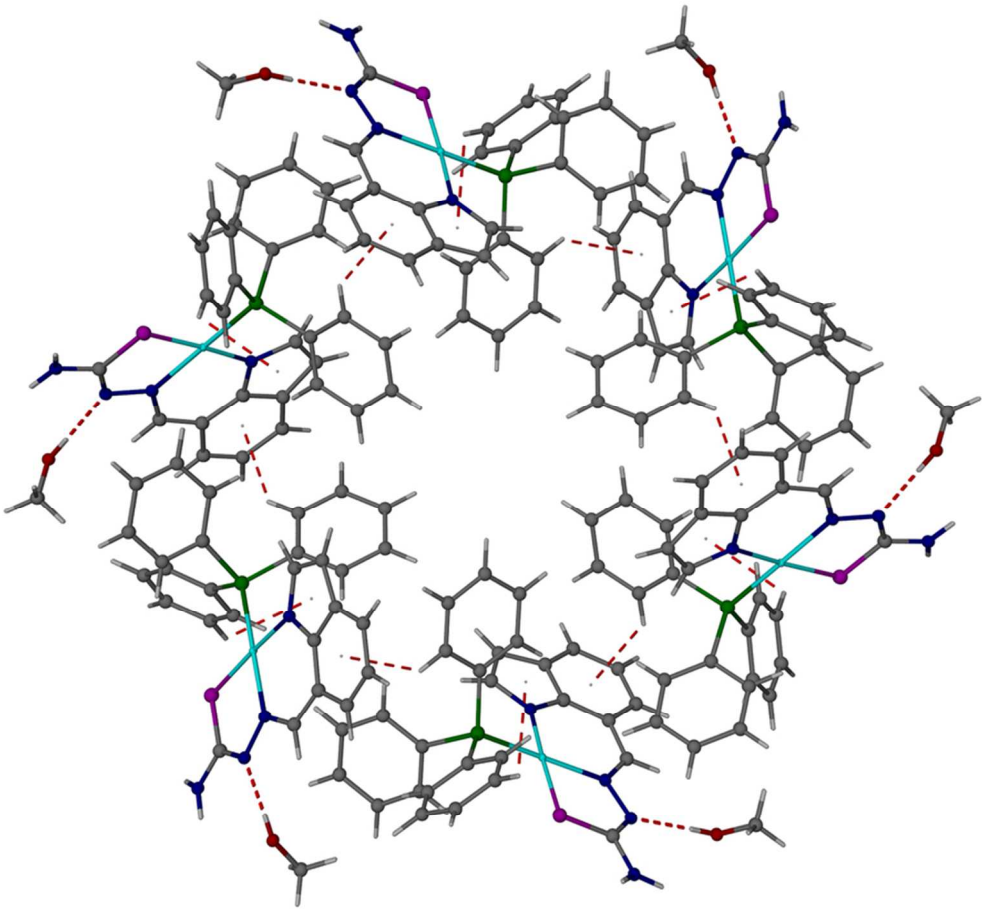

Fig. 8 Crystal packing view of Pt(L)(PPh3).0.75MeOH, showing channels along the c-axis. Hydrogen bonds are depicted as red dashed lines.
76x70mm (300 x 300 DPI)

Dalton Transactions Accepted Manuscript

View Article Online
DOI: 10.1039/C3DT53032A

Published on 26 November 2013. Downloaded by University of Malaya on 08/01/2014 07:12:34.

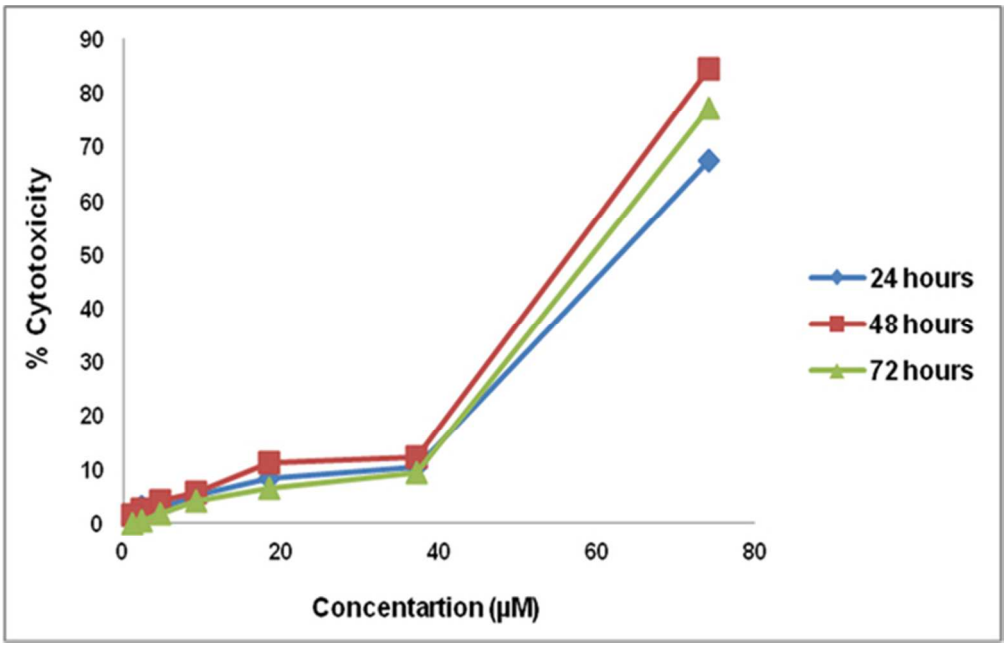

Fig. 9 Cytotoxicity effect of Pt(L)(PPh3) on normal liver WRL-68 cells
52x33mm (300 x 300 DPI)

Dalton Transactions Accepted Manuscript

View Article Online
DOI: 10.1039/C3DT53032A

Published on 26 November 2013. Downloaded by University of Malaya on 08/01/2014 07:12:34.

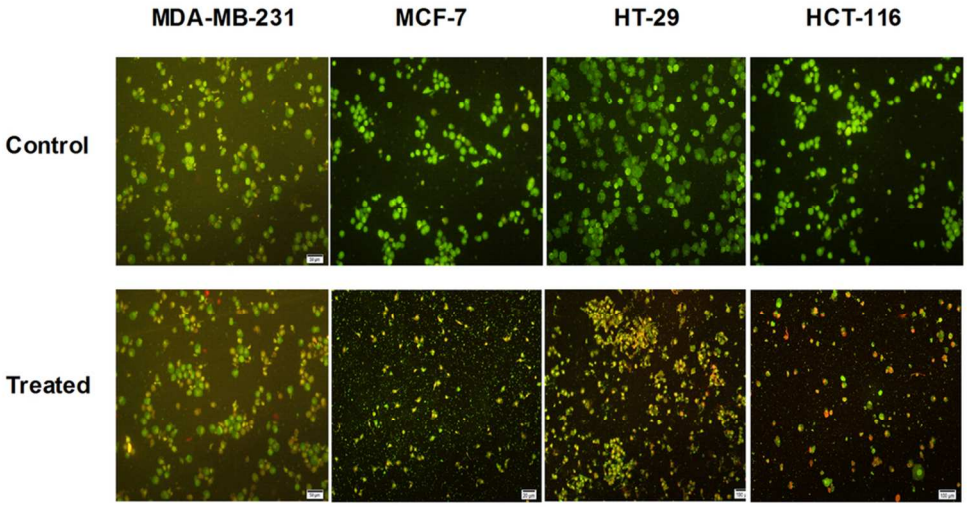

Fig. 10 Fluorescent microscopy of AO/PI stained cancer cells. The first row shows the cells without any treatment and the second row shows the cells after treatment with IC50 concentrations of Pt(L)PPh3 for 48 h. Cells with intact membrane are stained green. Apoptotic cells appear in orange-yellow and the necrotic cells are stained red.
90x48mm (300 x 300 DPI)

Dalton Transactions Accepted Manuscript

View Article Online
DOI: 10.1039/C3DT53032A

Published on 26 November 2013. Downloaded by University of Malaya on 08/01/2014 07:12:34.

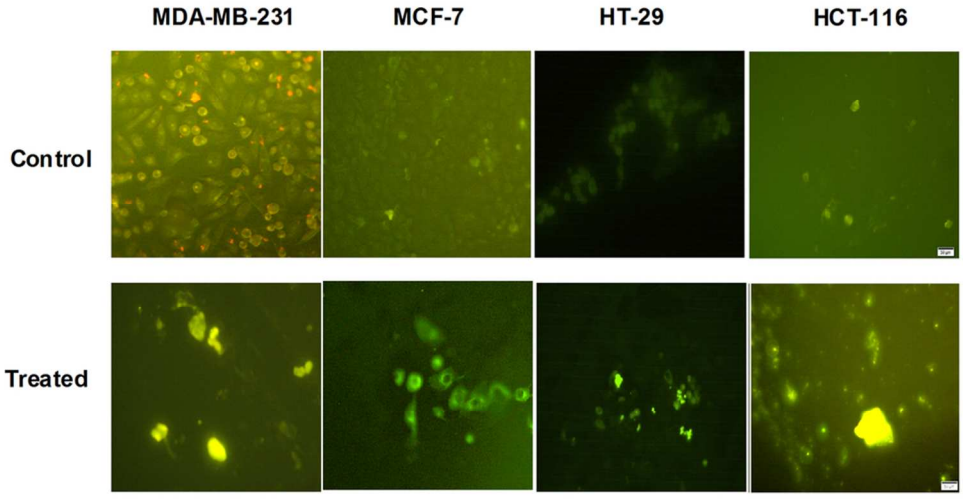

Fig. 11 Fluorescence microscopy of the cancer cells stained by FITC-annexin V. The first row shows the cells without any treatment and the second row shows the cells treated with Pt(L)PPh3 at IC50 concentraions for 48 h. FITC-annexin V positive cells show bright green fluorescence.
88x46mm (300 x 300 DPI)

Dalton Transactions Accepted Manuscript

View Article Online
DOI: 10.1039/C3DT53032A

Published on 26 November 2013. Downloaded by University of Malaya on 08/01/2014 07:12:34.

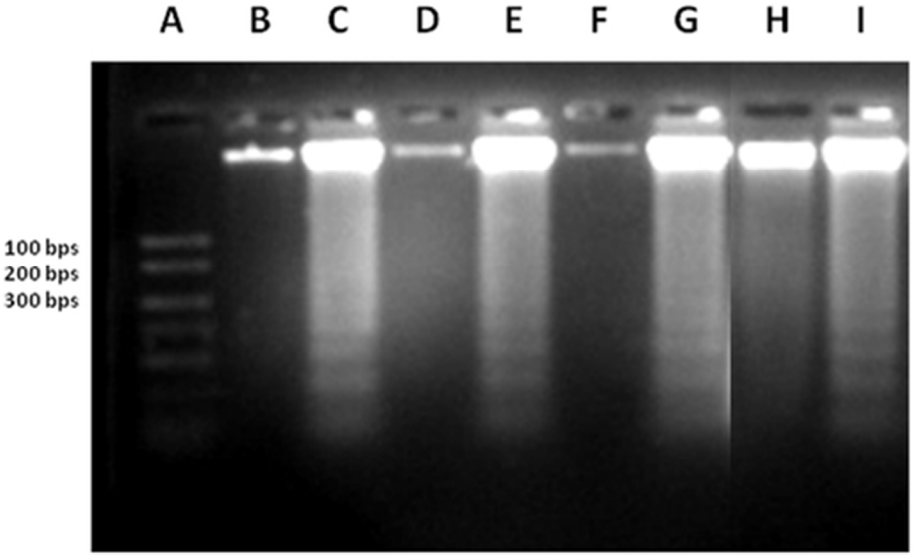

Fig. 12 Gel electrophoresis of apoptotic DNA fragmentation. Lane A: 1000 bp molecular weight marker; lane B: untreated MDA-MB-231 cells; lane C: treated MDA-MB-231 cells; lane D: untreated MCF-7 cells; lane E: treated MCF-7 cells; lane F: untreated HT-29 cells; lane G: treated HT-29 cells; lane H: untreated HCT-116 cells; lane I: treated HCT-116 cells.
47x27mm (300 x 300 DPI)

Dalton Transactions Accepted Manuscript

View Article Online
DOI: 10.1039/C3DT53032A

Published on 26 November 2013. Downloaded by University of Malaya on 08/01/2014 07:12:34.

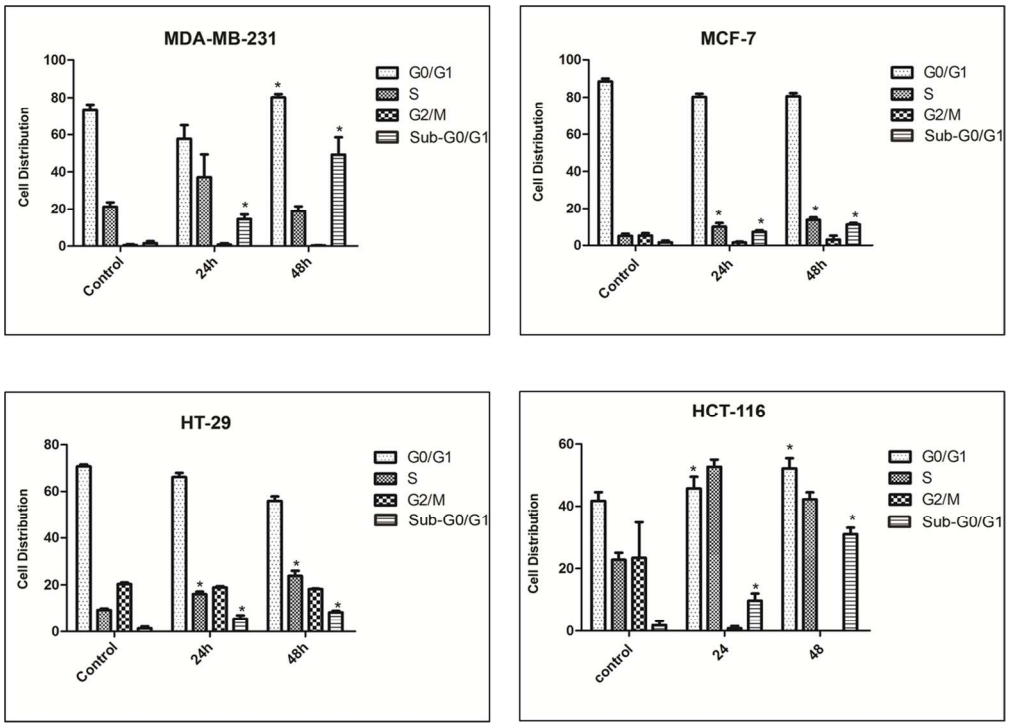

Fig. 13 Flow cytometric analysis of cell cycle distribution in the four cancer cell lines treated with IC50 concentrations of Pt(L)PPh3 for 24 and 48 h. Data were shown as Mean ± SEM. * ρ < 0.05 vs. controls.
122x87mm (300 x 300 DPI)

Dalton Transactions Accepted Manuscript

View publication stats